ACS OMEGA

http://pubs.acs.org/journal/acsodf

Article

Geochemical and Mineralogical Characteristics of the Li–Sr-Enriched Coal in the Wenjiaba Mine, Guizhou, SW China

Fangpeng Du,* Shuzheng Ning, Junwei Qiao, Furong Tan, Xiaochen Zhao, Weiguo Zhang, Congcong Li, Zheng Luo, and Xiaoyuan He

Cite This: *ACS Omega* 2021, 6, 8816–8828

Read Online

ACCESS | Metrics & More | Article Recommendations

ABSTRACT: This paper reports the mineralogical and geochemical compositions of C6 coal in the Late Permian Longtan Formation of the Wenjiaba Mine, Northern Guizhou in southwest (SW) China. The geochemical and mineralogical studies are the basis for the potential recovery of critical metals. The Longtan Formation, which is one of the major coal-bearing strata in SW China, contains dozens of coal seams. C6 coal is the main mineable coal seam in the Wenjiaba Mine and the whole coalfield. Proximate and ultimate analyses, inductively coupled plasma mass spectrometry (ICP-MS) and X-ray fluorescence (XRF) spectrometry on trace and major element concentrations, and X-ray diffraction and SEM-EDS analyses were carried out. Results suggest that this anthracite coal is characterized by low ash yield and medium sulfur content. The minerals are mainly composed of clay minerals (kaolinite, chlorite, illite, and mixed-layer illite/smectite), pyrite, and carbonates. Lithium is significantly enriched in C6 coal, with an average of 124 μg/g, and it has a higher concentration in the lower portion of the coal seam than that in the upper one. Strontium is significantly enriched in samples WJB-05 and WJB-06, with concentrations of 3030 and 4580 μg/g, respectively, but it is normal or just slightly enriched in other benches of C6 coal. Additionally, Cu, Nb, and Ta are slightly enriched in the coal. Lithium, dominantly hosted by kaolinite in C6 coals, has a recovery potential. Celestine is one of the major Sr-bearing minerals in C6 coal.

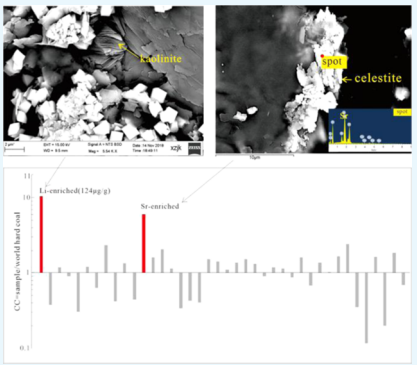

1. INTRODUCTION

The concentrations of critical metals in coal have attracted much attention due to their recovery potential and environmental concerns.[1−9] The Late Permian coals in southwest (SW) China are well known for their multienrichment of critical elements, such as V, U, Cr, Se, and rare-earth elements (REEs),[10−12] and even toxic/hazardous elements such as F, Hg, and Pb.[13] Several types of enrichment of trace element assemblages (i.e., U−Re−V−Cr−Sc and Nb−Zr−REY) were proposed.[11,12] Lithium- and Sr-rich type, however, have not been previously discovered and reported in the Late Permian coals in SW China.[14] Lithium is considered a significant potential energy metal because it is not only the key material of Li batteries but also used as a stabilizer in nuclear fusion reactors.[15,16] The average concentrations of Li and Sr are 12 and 100 μg/g in world hard coals, respectively.[17,18]

Lithium is one of the most highly investigated critical metals in Chinese coals. The Late Carboniferous−Early Permian coals in the north of North China Craton are the most well-known Li-rich coals.[19−22] The concentration of Li in No. 6 coal of the Heidaigou Mine, Jungar Coalfield, Inner Mongolia is 657 μg/g, and the concentration in No. 9 coal of the Anjialing Mine, Pingshuo Coalfield, Shanxi reaches as high as 840 μg/g.[21] In addition to the above well-known mining areas, other coalfields also bear Li-rich coals, such as the Jincheng and Huoxi Coalfields, with a Li concentration of approximately 120 μg/g.[23] The Late Permian coal in the Southeastern Chongqing Coalfield and the Fusui Coalfield in Guangxi are the specific regions with Li enrichment.[24−26] Lithium is always considered to be hosted by micas and clays in sedimentary rocks[19−21] and partially associated with organic matter.[27] Finkelman et al. concluded that 90% Li is associated with the clays and micas in high-rank coals, while the remainder is associated with the organics.[28−30] Strontium has both organic and inorganic associations in high-rank coals, and inorganic-associated Sr occurred as phosphates, barite, celestine, carbonates, strontianite, and clays.[28−35]

The geochemical and mineralogical characteristics of C6 coal in the Upper Permian Longtan Formation from the Wenjiaba Mine in Guizhou Province were reported in this paper with an emphasis on the geochemistry of Li and Sr. The Longtan Formation is one of the major coal-bearing strata in SW China

Received: November 21, 2020
Accepted: February 24, 2021
Published: March 22, 2021

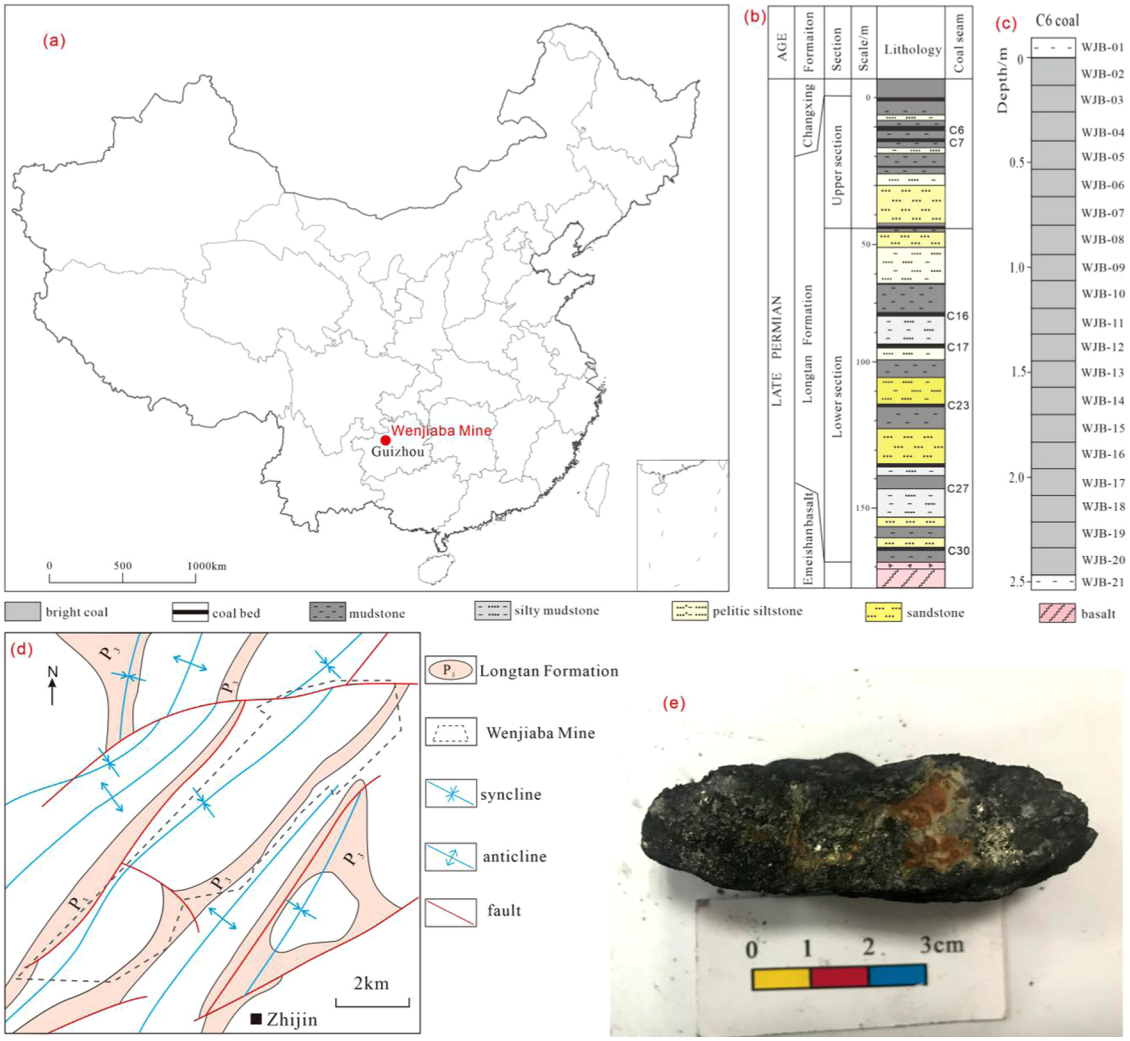

Figure 1. (a) Location of the Wenjiaba Mine, (b) generalized stratigraphic section of the Longtan Formation, (c) sampling section of C6 coal, (d) generalized geological map of the Wenjiaba Mine, and (e) photo of pyrite nodule in sample WJB-08.

Table 1. Proximate and Ultimate Results of the Wenjiaba Coal Samples (%)[a]

sample	M_{ad}	A_d	V_{daf}	$S_{t,d}$	C_{daf}	H_{daf}	N_{daf}	sample	M_{ad}	A_d	V_{daf}	$S_{t,d}$	C_{daf}	H_{daf}	N_{daf}
WJB-02	2.1	19.6	8.0	1.8	89.9	3.2	1.3	WJB-12	2.0	11.7	7.4	0.9	90.7	3.1	1.4
WJB-03	1.9	18.5	7.4	2.5	90.0	3.2	1.3	WJB-13	1.7	11.1	7.1	0.9	90.8	3.4	1.3
WJB-04	1.9	25.7	9.4	0.8	88.9	3.5	1.3	WJB-14	1.8	15.2	8.0	4.1	79.3	2.8	1.2
WJB-05	2.9	13.5	7.6	2.0	91.3	3.1	1.3	WJB-15	1.9	11.6	7.6	3.6	90.2	2.9	1.4
WJB-06	1.6	11.0	7.4	1.7	90.4	3.2	1.3	WJB-16	1.7	10.2	6.8	2.1	91.6	3.1	1.3
WJB-07	2.1	8.4	7.3	0.8	90.7	3.1	1.4	WJB-17	1.8	5.6	6.5	1.1	91.7	3.0	1.3
WJB-08	1.3	41.0		25.9	62.7	2.3	0.9	WJB-18	1.7	6.2	6.6	1.6	92.0	3.0	1.2
WJB-09	2.0	23.2	10.3	2.7	86.1	3.4	1.2	WJB-19	1.5	7.3	6.5	1.1	91.8	3.1	1.2
WJB-10	2.0	9.2	6.9	1.4	90.5	3.2	1.4	WJB-20	1.7	32.2	10.1	1.6	88.5	3.5	1.4
WJB-11	2.2	13.9	7.6	0.8	91.0	3.2	1.3	average without WJB-08	1.9	14.1	7.7	1.8	89.7	3.2	1.3

[a] M_{ad}, moisture (air-dry basis); A_d, ash yield (dry basis); V_{daf}, volatile matter (dry and ash-free basis); $S_{t,d}$, total sulfur (dry basis); C_{daf}, carbon; H_{daf}, hydrogen; N_{daf}, nitrogen.

and contains abundant coal resources. C6 coal is not only the main workable bed in the Wenjiaba Mine but also a major mineable coal bed in the whole coalfield. The geochemical and mineralogical studies may promote the recovery of critical metals, exemplified by Li in C6 coal, and the study will be conducive to the prevention of potential pollution during the utilization of Wenjiaba coal.

2. GEOLOGICAL SETTINGS

The Wenjiaba Mine is located in Zhijin City, Northern Guizhou Province of SW China (Figure 1a). It is one of the mines in Zhina Coalfield, which is located at the Northern Guizhou uplift in the Yangtze Platform.[36] A series of northeastern trending fold structures control the distribution of coalfields in the Northern Guizhou uplift (Figure 1d).

https://doi.org/10.1021/acsomega.0c05663
ACS Omega 2021, 6, 8816−8828

Table 2. Content of Major Element Oxides in the C6 Coal Samples (wt %; on Whole Coal Basis)

sample	SiO_2	TiO_2	Al_2O_3	Fe_2O_3	MgO	CaO	Na_2O	K_2O	LOI
WJB-02	11.5	0.21	4.2	2.3	0.22	0.11	0.27	0.24	80.4
WJB-03	10.1	0.16	4.0	3.1	0.15	0.11	0.26	0.22	81.5
WJB-04	13.9	0.20	9.0	0.90	0.25	0.31	0.39	0.33	74.3
WJB-05	6.5	0.22	2.9	2.2	0.04	0.28	0.22	0.14	86.5
WJB-06	4.5	0.13	2.5	1.6	0.07	0.61	0.19	0.08	89
WJB-07	4.1	0.10	2.6	0.55	0.06	0.23	0.16	0.08	91.6
WJB-08	3.9	0.21	1.6	32.9	0.01	0.37	0.10	0.07	59.0
WJB-09	10.5	0.20	8.2	3.2	0.03	0.05	0.20	0.16	76.8
WJB-10	3.8	0.11	3.2	1.1	0.03	0.17	0.19	0.09	90.8
WJB-11	6.3	0.16	5.0	0.50	0.12	0.39	0.28	0.25	86.1
WJB-12	5.4	0.16	4.4	0.70	0.05	0.11	0.23	0.16	88.3
WJB-13	5.1	0.14	4.0	0.70	0.08	0.13	0.25	0.16	88.9
WJB-14	4.8	0.20	3.6	5.0	0.01	0.4	0.23	0.11	84.8
WJB-15	3.6	0.51	2.9	4.0	0.01	0.05	0.19	0.07	88.4
WJB-16	3.7	0.61	2.9	2.1	0.03	0.02	0.21	0.07	89.8
WJB-17	2.2	0.06	1.8	0.88	0.02	0.11	0.13	0.04	94.4
WJB-18	2.1	0.07	1.6	1.6	0.08	0.22	0.12	0.05	93.8
WJB-19	2.9	0.15	2.3	1.1	0.10	0.09	0.14	0.09	92.8
WJB-20	14.4	1.0	10.3	3.1	0.54	0.07	0.54	0.74	67.8
C6 coals	6.3	0.24	4.0	3.6	0.10	0.20	0.23	0.17	84.5
Chinese coals[18]	8.5	0.33	6.0	4.9	0.22	1.2	0.16	0.19	

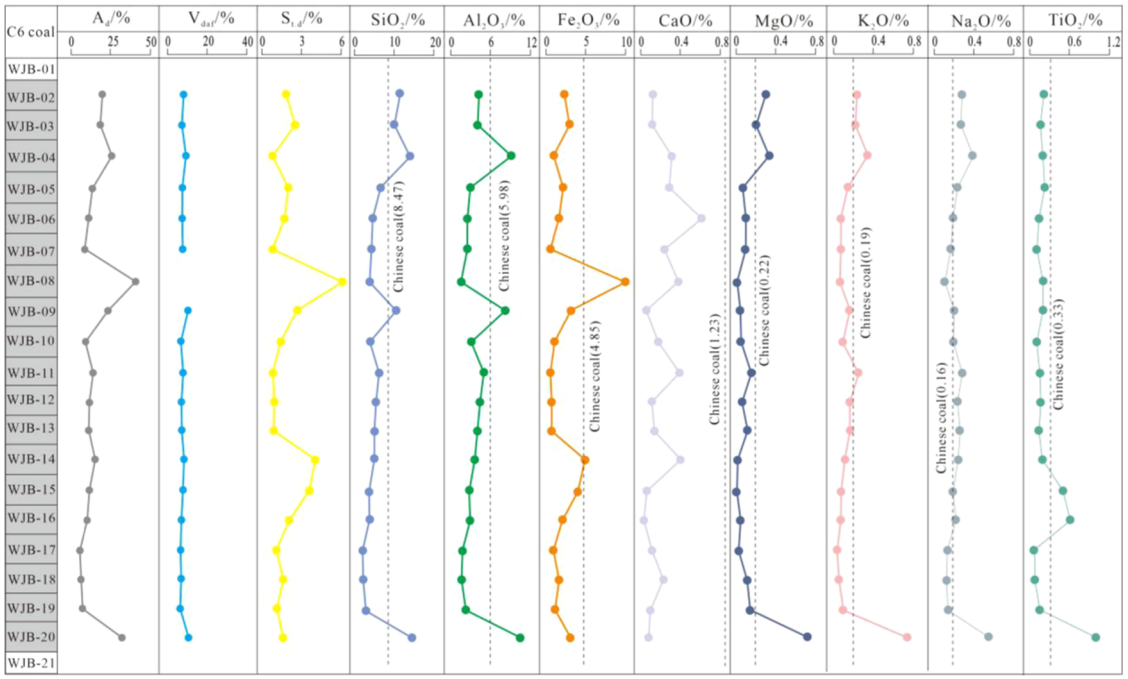

Figure 2. Vertical variations of ash yield, volatile matter, total sulfur, and major elements across the C6 coal section.

The Upper Permian strata in this area include the Emeishan basalt, Longtan Formation, and Changxing Formation. The Emeishan basalt, which is widespread in SW China, dominantly influenced the multienrichment of critical elements in the Late Permian coals.[37] The Longtan Formation is the major coal-bearing stratum in the Wenjiaba Mine, even in SW China, with a thickness of 300 m and 30 coal seams (Figure 1b). It was deposited in an alternate marine−continental environment,[38] and the lithologic associations are sandstone, silt, mudstone, and coal. Coal seams were numbered from top to bottom of the Longtan Formation, and coal seams C6, C7, C16, C23, C27, and C30 are the main minable coal seams in the Wenjiaba Mine; however, C6 coal is the main working bed at present, with a thickness of 2.5 m.

3. SAMPLES AND ANALYTICAL METHODS

The analyzed samples were collected from the C6 coal underground workings of the Wenjiaba Mine; 18 coal samples and 2 mudstone samples were collected from the roof to the floor using a channeling sampling method (Figure 1c). Furthermore, massive pyrite nodules that occurred in this seam represented by sample WJB-08 were also collected (Figure 1e).

https://doi.org/10.1021/acsomega.0c05663
ACS Omega 2021, 6, 8816−8828

Table 3. Trace Element Concentrations in the Roof, Floor, and Coals from the Wenjiaba C6 Coal Seam (on Whole Coal/Rock Basis, μg/g)

element	concentration (μg/g)											
	WJB-01	WJB-02	WJB-03	WJB-04	WJB-05	WJB-06	WJB-07	WJB-08	WJB-09	WJB-10	WJB-11	WJB-12
Li	95	82	93	195	95	108	109	46	163	140	173	168
Be	4.7	0.74	0.53	1.3	0.46	0.43	0.48	0.36	1.1	0.5	0.8	0.77
Sc	9.0	5.0	4.1	5.8	5.9	3.1	4.5	1.6	4.5	3.0	4.8	4.7
Cr	21.2	14	13	9.5	19	11	14	11	12	7.8	11	13
Mn	100	45	26	32	17	14	16	64	26	11	21	15
Co	1.5	4.8	3.8	2.8	4.9	4.8	5.1	16	4.2	5.5	5.6	5.5
Ni	7.5	14	8.0	3.7	4.2	4.1	5.7	37	6.1	5.0	5.4	5.4
Cu	11	11	18	12	79	14	17	114	21	17	25	19
Zn	27	11	8.0	9.7	7.4	4.6	8.1	25	8.1	4.3	7.0	6.4
Ga	36	6.5	6.9	14	5.1	3.8	6.9	3.1	12	5.2	9.0	7.6
Rb	86	9.0	7.7	11	5.1	3.0	4.7	4.6	6.3	3.1	8.8	6.0
Sr	514	238	115	374	3030	4580	742	224	125	176	137	258
Y	14	16	12	11	13	12	13	6.7	13	14	19	16
Nb	15	5.9	6.4	10	5.9	3.4	6.6	3.7	8.5	3.5	7.1	6.3
Mo	0.88	1.4	4.5	0.56	1.3	0.67	0.65	21	1.6	0.82	0.41	0.31
Cd	0.04	0.03	0.05	0.01	0.03	0.02	0.02	0.46	0.05	0.04	0.06	0.06
Cs	4.9	0.62	0.48	0.69	0.39	0.24	0.40	0.62	0.54	0.26	0.60	0.47
Ba	834	83	68	117	45	38	47	28	58	23	90	58
La	25	19	12	20	14	22	15	3.6	17	13	15	21
Ce	55	33	26	38	28	35	28	7.1	32	24	32	37
Pr	6.6	3.7	3.2	4.4	3.5	4.1	3.3	1.2	3.6	2.9	3.8	4.2
Nd	24	15	12	17	14	17	15	4.5	14	11.6	15	16
Sm	4.0	2.9	2.3	3.1	2.5	2.8	2.7	1.4	2.7	2.3	3.0	3.0
Eu	0.40	0.45	0.4	0.43	0.4	0.51	0.61	0.31	0.5	0.36	0.49	0.49
Gd	2.5	2.4	1.9	2.1	2.1	2.5	2.2	1.4	2.1	2.0	2.6	2.6
Tb	0.4	0.42	0.3	0.34	0.34	0.36	0.34	0.22	0.34	0.38	0.50	0.43
Dy	2.3	2.7	2.3	2.2	2.2	2.1	2.1	1.1	2.3	2.5	3.5	2.7
Ho	0.5	0.53	0.46	0.43	0.46	0.39	0.41	0.23	0.49	0.5	0.72	0.53
Er	1.6	1.6	1.3	1.3	1.5	1.2	2.0	0.50	1.5	1.5	2.1	1.6
Tm	0.28	0.25	0.20	0.22	0.2	0.16	0.18	0.10	0.23	0.22	0.32	0.24
Yb	1.8	1.6	1.4	1.4	1.4	1.0	1.2	0.55	1.5	1.5	2.0	1.6
Lu	0.30	0.24	0.20	0.20	0.2	0.15	0.17	0.09	0.22	0.21	0.29	0.23
Ta	2.1	0.46	0.52	1.5	0.49	0.26	0.55	0.15	1.0	0.27	0.73	0.73
W	0.96	0.32	0.34	0.51	0.53	0.28	0.40	0.15	0.39	0.23	0.30	0.34
Tl	0.23	0.05	0.08	0.04	0.05	0.03	0.02	0.69	0.05	0.02	0.03	0.02
Pb	4.6	9.1	27	4.3	13	3.1	2.2	70	26	11	3.2	4.3
Bi	0.53	0.22	0.18	0.39	0.16	0.1	0.16	0.13	0.42	0.14	0.29	0.25
Th	22	5.3	6.7	23	4.1	2.2	4.9	2.4	13	3.3	8.2	7.7
U	5.8	3.8	2.7	3.6	1.1	0.47	1.3	0.70	3.2	1.1	2.8	1.7
	WJB-13	WJB-14	WJB-15	WJB-16	WJB-17	WJB-18	WJB-19	WJB-20	WJB-21	average	world hard coal average[17]	
Li	169	174	145	142	85	73	84	116	149	124	12	
Be	0.55	0.50	0.44	0.46	0.31	0.38	0.46	1.1	4.19	0.61	1.6	
Sc	3.9	3.3	3.9	4.3	2.0	2.1	4.6	17	40	4.7	3.9	
Cr	8.6	11	19	26	6.6	7.1	11	50	151	14	16	
Mn	12	28	15	10	8.8	10	10	25	98	21	70	
Co	3.3	6.1	5.6	8.7	6.9	5.8	5.5	13	61	6.2	5.1	
Ni	3.8	5.4	4.8	5.5	4.4	4.3	5.7	23	56	8.2	13	
Cu	13	37	46	42	30	26	39	123	143	37	16	
Zn	6.7	10	9.3	9.1	3.8	6.0	9.0	29	63	9.6	23	
Ga	8.2	7.4	6.2	6.5	4.9	4.6	5.3	25	48	7.8	5.8	
Rb	6.1	5.0	3.7	3.6	1.9	1.7	3.1	23	39	6.2	14	
Sr	128	139	89	91	156	274	734	998	778	664	110	
Y	11	11	14	14	11	9.8	20	23	52	14	8.4	
Nb	5.0	5.2	14	17	2.0	1.7	4.2	28	105	7.6	3.7	
Mo	0.2	3.7	3.3	1.6	0.51	1.4	0.6	3.3	5.0	2.5	2.2	
Cd	0.04	0.14	0.10	0.09	0.07	0.08	0.06	0.09	0.12	0.07	0.22	
Cs	0.39	0.39	0.33	0.26	0.15	0.14	0.24	0.93	1.8	0.43	1	
Ba	58	37	35	44	15	12	26	277	841	61	150	

https://doi.org/10.1021/acsomega.0c05663
ACS Omega 2021, 6, 8816−8828

Table 3. continued

element	concentration (μg/g)										
	WJB-13	WJB-14	WJB-15	WJB-16	WJB-17	WJB-18	WJB-19	WJB-20	WJB-21	average	world hard coal average[17]
La	10	11	15	17	13	15	15	51	77	17	11
Ce	20	22	27	29	26	32	34	109	160	33	23
Pr	2.4	2.5	3.3	3.5	3.1	3.8	4.2	13	20	3.9	3.5
Nd	9.3	10	13	15	14	18	19	61	82	16	12
Sm	1.9	2.0	2.4	2.6	2.5	3.2	3.6	11	15	3.1	2
Eu	0.4	0.41	0.49	0.54	0.56	0.76	0.98	2.8	3.4	0.62	0.47
Gd	1.5	1.8	2.1	2.2	2.2	2.7	3.3	6.7	13	2.5	2.7
Tb	0.26	0.3	0.4	0.4	0.33	0.35	0.53	0.79	2.1	0.38	0.32
Dy	1.8	2.0	2.3	2.5	2.0	1.9	3.3	4.3	13	2.4	2.1
Ho	0.36	0.38	0.45	0.48	0.35	0.32	0.63	0.86	2.3	0.47	0.54
Er	1.2	1.2	1.4	1.5	1.1	0.95	1.9	2.7	6.0	1.5	0.93
Tm	0.18	0.18	0.21	0.23	0.15	0.12	0.26	0.38	0.84	0.21	0.31
Yb	1.1	1.2	1.4	1.4	1.0	0.80	1.7	2.5	5.0	1.4	1.0
Lu	0.17	0.18	0.2	0.21	0.15	0.12	0.24	0.37	0.72	0.20	0.2
Ta	0.47	0.44	1.1	1.3	0.14	0.14	0.31	2.4	7.1	0.68	0.28
W	0.23	0.24	0.98	1.1	0.08	0.06	0.15	0.80	2.6	0.39	1.1
Tl	0.02	0.07	0.05	0.02	0.01	0.02	0.02	0.12	0.22	0.07	0.63
Pb	4.0	25	18	8.8	2.7	3.1	3.1	4.7	11	13	7.8
Bi	0.17	0.25	0.16	0.18	0.11	0.07	0.08	0.23	0.20	0.19	0.97
Th	6.4	5.2	3.8	4.3	1.3	1.1	2.0	10	16	6.1	3.3
U	1.6	1.5	1.0	1.0	0.43	0.33	0.83	2.9	6.1	1.7	2.4

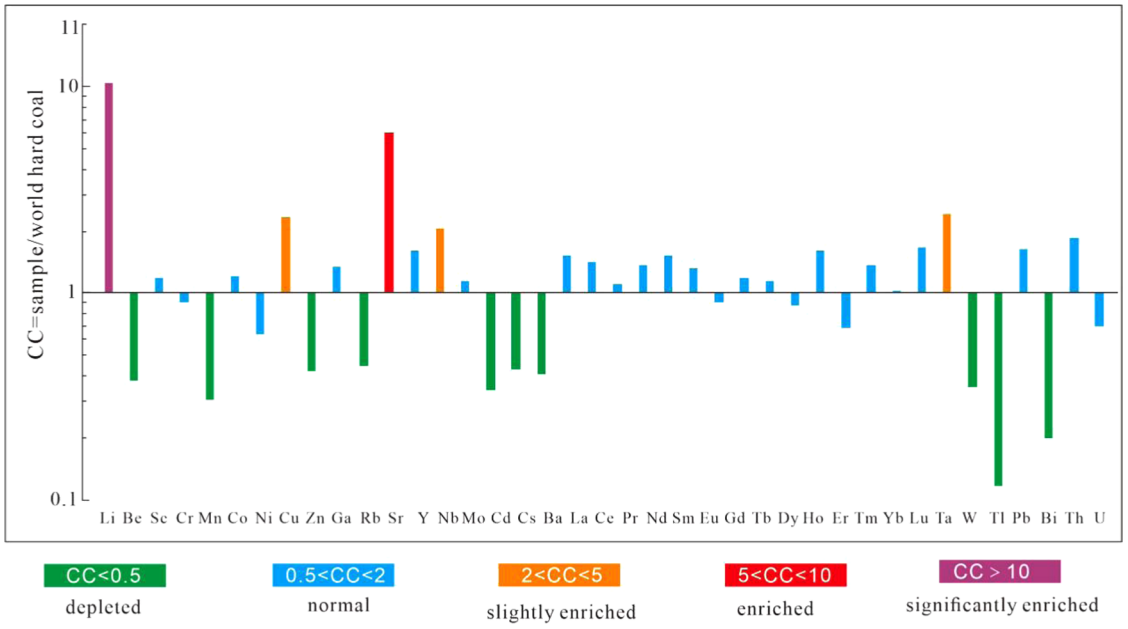

Figure 3. Concentration coefficients of trace elements in C6 coal, compared to the world hard coals.[17]

Proximate analyses (i.e., A_d, M_{ad}, and V_{daf}) of the coal samples were conducted in accordance with the Chinese national standard GB/T 30732-2014,[39] and the total sulfur content was determined according to the GB/T 214-2007.[40] The C, H, and N contents of the coal samples were determined with a CTCH500 Hydrocarbon Analyzer and Azotometer. Bulk samples were crushed and ground to 200 mesh and acid-digested by HNO_3/HF + H_3BO_3 for trace elemental analysis. Inductively coupled plasma mass spectrometry (ICP-MS, ICAP-Qc) was used to determine the concentrations of trace elements and rare-earth elements (REEs) in the samples. Chinese national certified reference materials GBW11156 and GSD17-a were tested along with the samples to control the quality of trace element determination. Detection limits of trace elements by ICP-MS vary substantially. Strontium, Ba, and Cr have the highest detection limit of 5 μg/g. The detection limit of Li, Sc, and Zn is 1.0 μg/g, and for most trace elements, it ranges from 0.1 to 0.5 μg/g. The powdered coal samples were ashed at a high temperature of 815 ± 10 °C in advance for the determination of major element oxides. SiO_2, TiO_2, Al_2O_3, Fe_2O_3, MgO, CaO, Na_2O, and K_2O were determined by X-ray fluorescence (XRF) spectrometry. The ash-based oxides were recalculated to whole coal basis. Three coal samples (WJB-04, WJB-12, and WJB-19), which represent each part of C6 coal, were selected and ashed at a low temperature (<150 °C) using a Quorum K1050X Plasma Etcher. Mineralogical identification of the roof and floor rock

https://doi.org/10.1021/acsomega.0c05663
ACS Omega 2021, 6, 8816−8828

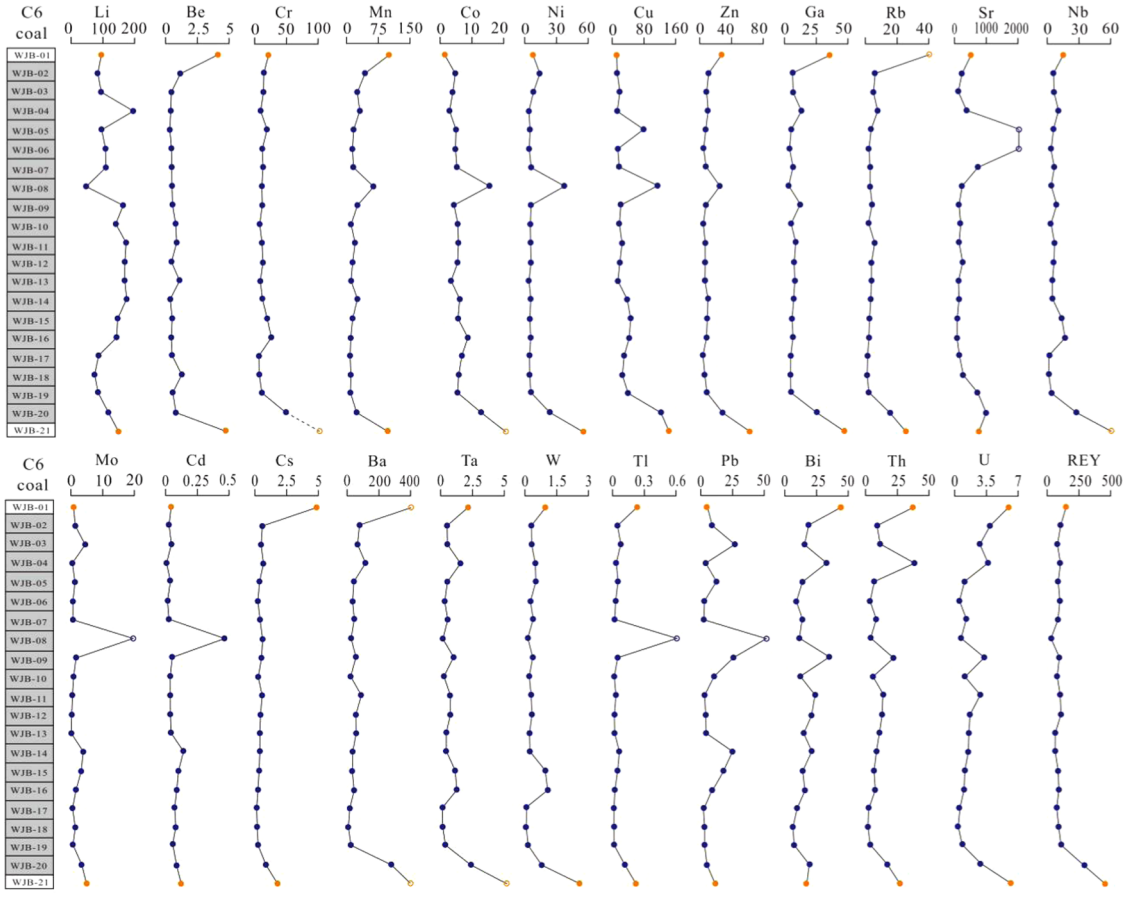

Figure 4. Vertical distributions of trace elements across the C6 coal section (empty point stands for being exceeding maximum values in the scale; REY = REE + Y).

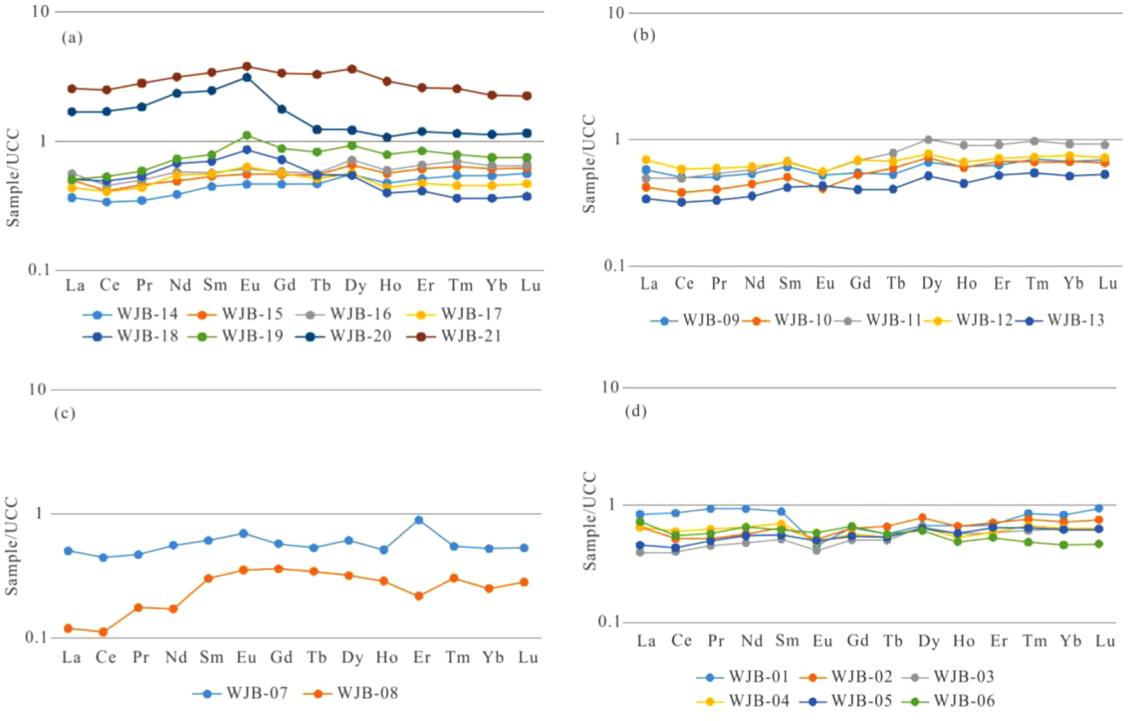

Figure 5. Rare-earth element distribution pattern of C6 coal normalized by the upper continental crust (UCC):[44] (a) samples WJB-21 to WJB-14, (b) samples WJB-13 to WJB-09, (c) samples WJB-08 to WJB-07, and (d) samples WJB-06 to WJB-01.

https://doi.org/10.1021/acsomega.0c05663
ACS Omega 2021, 6, 8816−8828

samples and the low-temperature ashed coal samples was performed by powder X-ray diffraction (XRD) using a D8 Discover with a stepwise scanning of 0.02°. The scanning range of the whole rock is 5−45° 2θ, and the clay was scanned three times with the scanning ranges of 2.5−15, 2.5−30, and 3−15° 2θ, respectively. The quantitative measures of whole rock and clay minerals were based on calculation software Clayquan and Rockquan, respectively, developed by Lin. The analysis is according to the industry standard in China (SY/T 5163-2010).[41] Prior to the SEM-EDS analyses, the coal grain samples were gold-coated. A field-emission scanning electron microscope (FE-SEM, SIGMA 300), in conjunction with energy-dispersive X-ray, was used to investigate the morphology of the minerals and to determine the distribution of some elements in coal samples WJB-05, WJB-11, WJB-12, and WJB-14.

4. RESULTS

4.1. Coal Chemistry. The ash yield was variable, ranging from 5.6 to 32.2%, with an average of 14.1%, indicating low ash coal in general.[42] The volatile matter content of the coal samples ranged from 7.4 to 10.3%, with an average of 7.7% (Table 1), representing low-volatile coal.[42] The total sulfur content ranged from 0.8 to 4.1%, with an average of 1.8%, indicating medium-sulfur coal.[42] Sample WJB-08 was significantly different from others in this coal seam, with a higher ash yield and total sulfur content and lower moisture and C, H, and N contents than other coal samples.

4.2. Geochemistry. *4.2.1. Major Oxides.* SiO_2 and Al_2O_3 were the main components (Table 2) of major element oxides in C6 coal, with average contents of 6.3 and 4.0%, respectively, which were lower than those in the common Chinese coals.[18] The concentrations of Fe_2O_3, MgO, TiO_2, K_2O, and CaO in C6 coal were also lower than those in common Chinese coals, whereas Na_2O was the single major oxide with a higher average content than Chinese coals. The variations of SiO_2, Al_2O_3, MgO, Na_2O, and K_2O contents across the sampling section resemble the ash yields, except WJB-08 (Figure 2). The Fe_2O_3 content variation in the section coincides with the sulfur content.

4.2.2. Trace Elements. Trace element concentrations in the coal samples and roof and floor rock samples of C6 coal are given in Table 3. Concentration coefficient (CC) is used to reflect the enrichment of trace elements in coals, which is calculated by samples investigated divided by averages for world hard coals.[43] The enrichment was classified into unusually enriched (CC > 100), significantly enriched (10 < CC < 100), enriched (5 < CC < 10), slightly enriched (2 < CC < 5), normal (0.5 < CC < 2), and depleted (CC < 0.5).[43]

Based on the CC of elements, Li is significantly enriched and Sr is enriched in the C6 coal, with average concentrations of 124 and 664 μg/g, respectively. C6 coal is also slightly enriched in Cu, Nb, and Ta, with average concentrations of 37, 7.6, and 0.68 μg/g, respectively. Beryllium, Mn, Zn, As, Rb, Cd, Cs, Ba, W, Tl, and Bi are depleted, and the remaining elements are in normal ranges (Figure 3).

Trace element concentrations of the coal samples were lower than those of roof and floor rock samples (Figure 4). Sample WJB-08 was also conspicuous in terms of vertical changes of certain trace elements, such as Co, Ni, Cu, Tl, and Pb (Figure 4). The variation of Li throughout the C6 coal was quite different from other elements. First, the concentrations of Li in coal and noncoal roof and floor samples are similar. Second, sample WJB-08 has the lowest Li content across the section, which is in sharp contrast to other elements with the maximum therein.

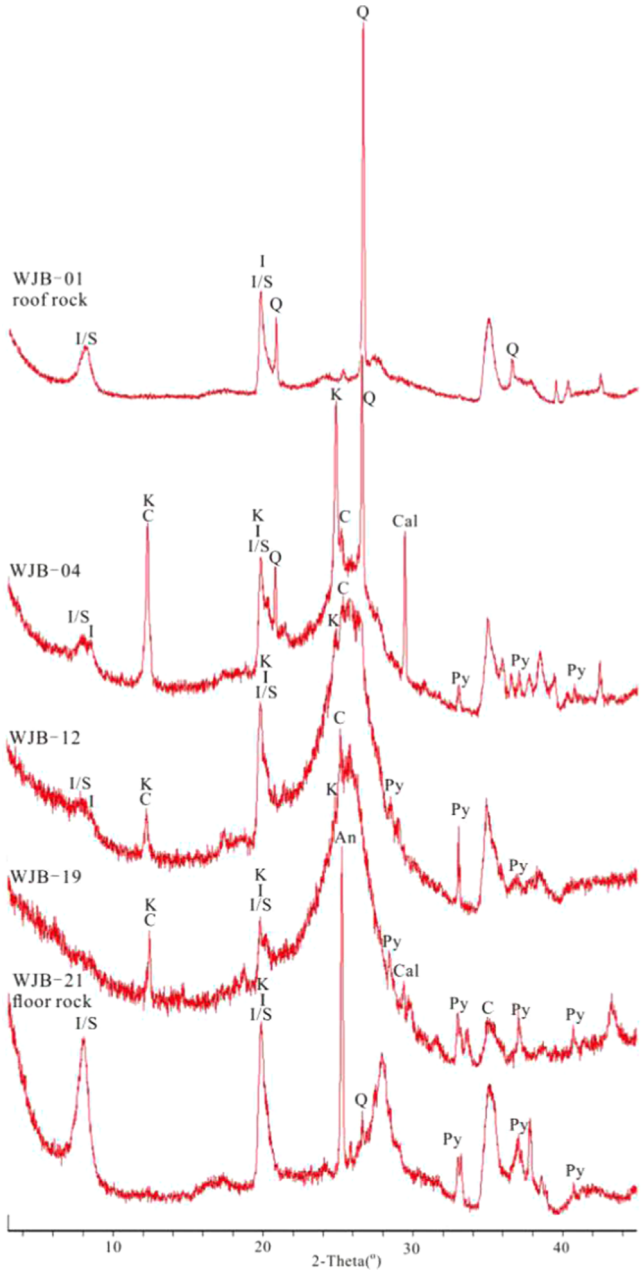

Figure 6. XRD patterns of the low-temperature ashed coal samples and roof and floor rock samples.

Additionally, Li concentrations are relatively high in the central part of the studied section. Sr is significantly enriched in samples WJB-05 and WJB-06, whereas Sr concentrations in the remaining samples are generally within the range of world hard coals.

4.2.3. Rare-Earth Elements. Rare-earth element concentrations were at the normal level in C6 coal compared to the world hard coals.[17] REEs were divided into three fractions, light REE (LREE, including La, Ce, Pr, Nd, and Sm), medium REE (MREE, including Eu, Gd, Tb, and Dy), and heavy REE (HREE, including Ho, Er, Tm, Yb, and Lu).[1]

REE distribution patterns normalized by the upper continental crust (UCC) differed in each portion of C6 coal.[43] The floor (WJB-21) was characterized by the positive Eu anomalies; the lowest portion of the coal inherited this feature. The positive Eu anomaly was increasingly weaker upward in turn from WJB-

https://doi.org/10.1021/acsomega.0c05663
ACS Omega 2021, 6, 8816−8828

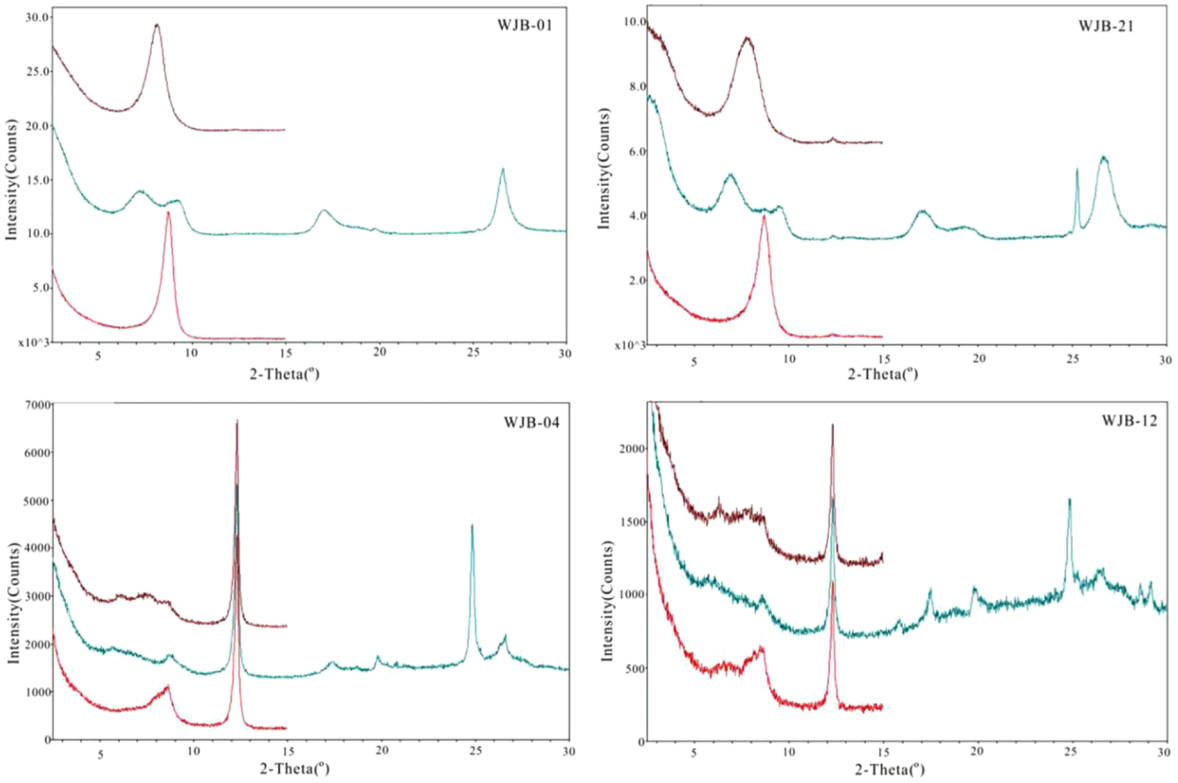

Figure 7. XRD patterns of clay minerals in the low-temperature ashed coal samples and roof and floor rock samples.

Table 4. Percentage of Minerals in the Low-Temperature Ashed Coal Samples and Roof and Floor Mudstone Samples[a]

		clay mineral				whole rock					
sample	LTA yield	kaolinite	chlorite	illite	I/S	total clay	quartz	feldspar	calcite	pyrite	anatase
WJB-01				1	99	85.6	14.1	0.3			
WJB-04	35.6	51	7	3	39	80.5	12.9		5.2	1.4	
WJB-08						2	15			83	
WJB-12	29.3	32	8	7	53	90	2.8			7.2	
WJB-19	28.7	8	61	6	25	91.2			1.4	7.4	
WJB-21		1		1	98	85	1			3.3	10.7

[a]I/S, illite/smectite.

20 to WJB-14 (Figure 5a). The middle portion of C6 coal from WJB-13 to WJB-09 was characterized by a negative Eu anomaly (Figure 5b). Sample WJB-08 has the lowest REE concentration across the C6 coal, and its distribution pattern was also uncommon (Figure 5c). Sample WJB-07 was characterized by the slightly positive Eu anomalies. The REE distribution patterns of coal samples WJB-06 to WJB-02 and the roof were present as negative Eu anomalies (Figure 5d).

4.3. Mineralogy. *4.3.1. X-Ray Diffraction Results.* X-ray diffraction data show that the minerals in the low-temperature ashed coal samples are mainly composed of quartz, pyrite, calcite, kaolinite, chlorite, illite, and mixed-layer illite/smectite (Figures 6 and 7). The percentages of each clay mineral were diverse (Table 4). The kaolinite content was high in samples WJB-04 and WJB-12 and low in WJB-19. On the contrary, the chlorite content was low in WJB-04 and WJB-12 but high in WJB-19. Clay minerals had also a major percentage in mudstone samples WJB-01 and WJB-21, but the composition of the clay minerals was different from that in the low-temperature ashed coal samples. The mixed-layer I/S was the dominant clay mineral in the mudstone samples, while kaolinite and chlorite were rare. Chamosite and clinochlore are the two common varieties of chlorite. The XRD patterns indicated that the chlorite variety in C6 coal was chamosite (Figure 7).[45] In addition, feldspar and anatase occurred in the roof and floor, respectively. Pyrite was the major component in pyrite nodules (WJB-08), consistent with our field macroscopical observations, and quartz was also identified in both coal samples and rock samples.

4.3.2. Minerals Observed by SEM-EDS. SEM-EDS analysis was carried out to determine the mineral morphology in C6 coal (Figure 8). Clay minerals were widely observed in C6 coals, which often occurred in filling the cell lumens of the inertinite macerals or voids of other macerals (Figure 8c). Chlorite (Figure 8d), kaolinite (Figure 8a), and illite/smectite (Figure 8c) were the major clay minerals. Celestine was found in sample WJB-05 (Figure 8d). Pyrite was one of the major minerals in C6 coal, occurring as both fine-grained single-crystal pyrite (Figure 8a) and framboidal grain (Figure 8b). The widespread clay minerals correspond to the high content of SiO_2 and Al_2O_3 in the coal, and the common pyrite contributes to the relatively high Fe_2O_3 and sulfur content in the coal.

https://doi.org/10.1021/acsomega.0c05663
ACS Omega 2021, 6, 8816−8828

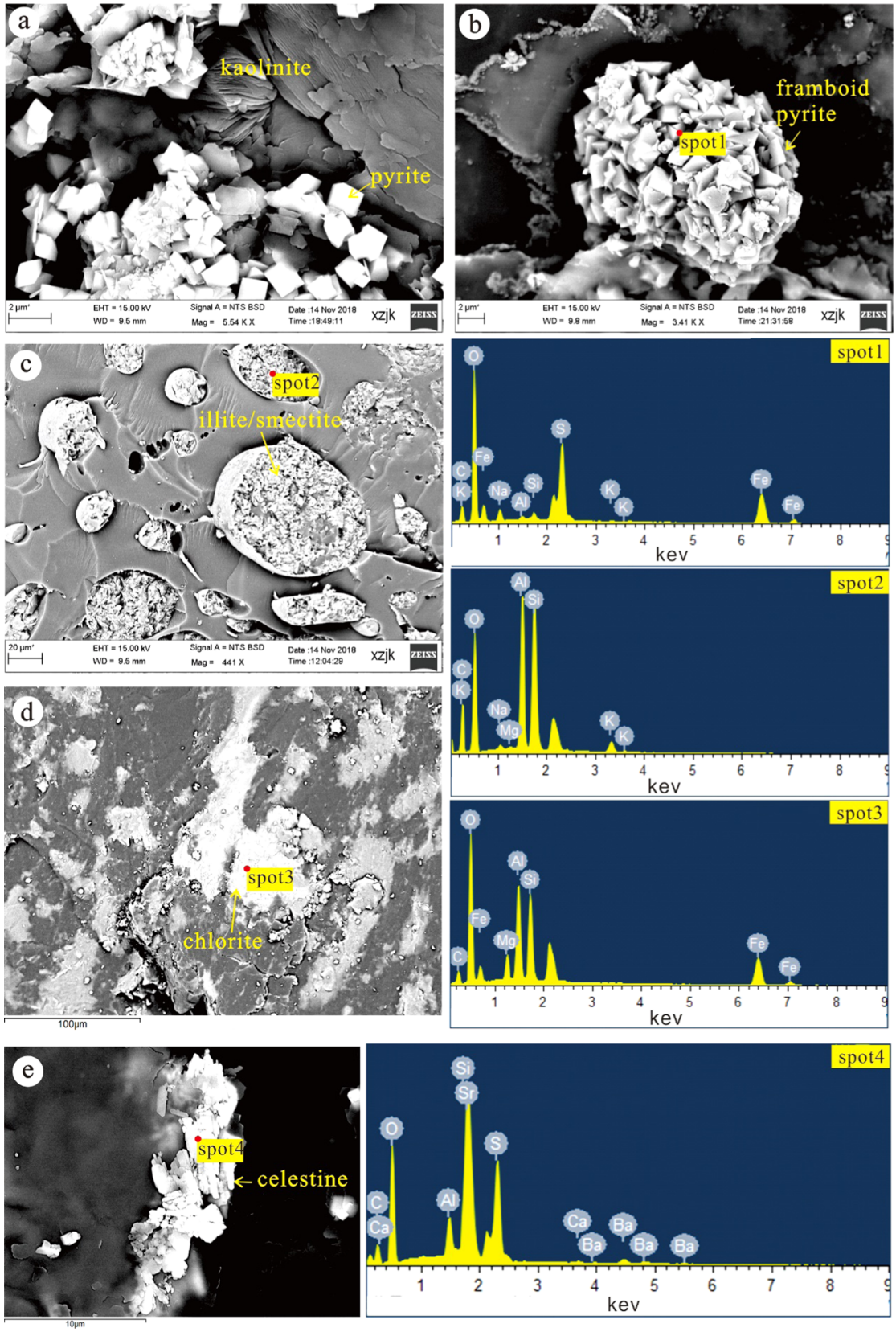

Figure 8. SEM images and EDS spectra of C6 coal in the Wenjiaba Mine, (a) kaolinite and pyrite in sample WJB-12, (b) framboid pyrite in sample WJB-12, (c) Fe-bearing illite/smectite in organic matter of sample WJB-11, (d) Mg- and Fe-bearing chlorite in sample WJB-14, and (e) Ca- and Ba-bearing celestine in sample WJB-05.

https://doi.org/10.1021/acsomega.0c05663
ACS Omega 2021, 6, 8816−8828

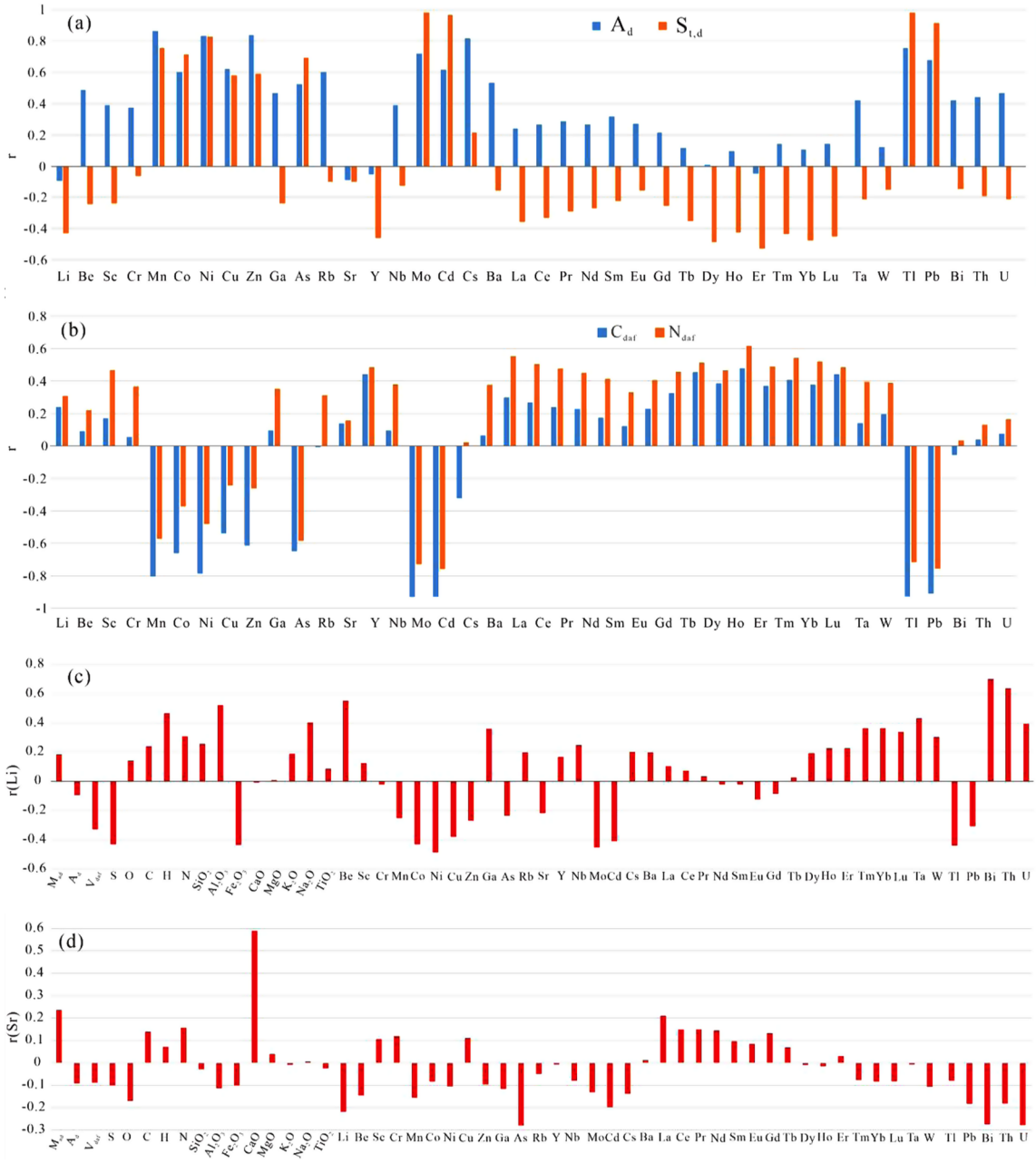

Figure 9. (a) Pearson correlations between trace elements and ash yield, total sulfur; (b) Pearson correlations between trace elements and C and N contents; (c) Pearson correlations between Li and moisture, ash yield, volatile matter, total sulfur, O, C, H, and N contents, and other elements; and (d) Pearson correlations between Sr and moisture, ash yield, volatile matter, total sulfur, O, C, H, and N contents, and other elements.

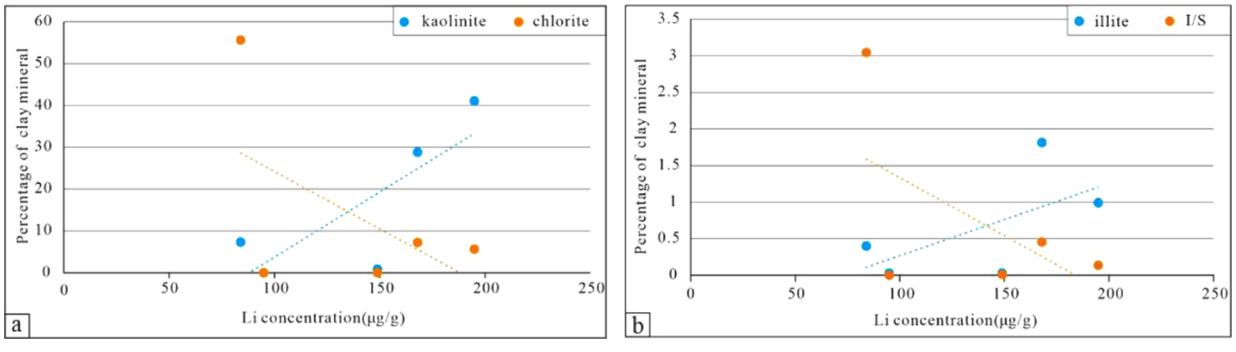

Figure 10. (a) Scatter plots of Li with kaolinite and chlorite and (b) scatter plots of Li with illite and I/S.

https://doi.org/10.1021/acsomega.0c05663
ACS Omega 2021, 6, 8816−8828

5. DISCUSSION

Statistical methods (e.g., Pearson correlation and cluster analysis) are commonly performed for determining the occurrence mode of trace elements, although they have some limitations. The elemental affinities support from direct methods (e.g., SEM-EDS) contribute to more accurate results.[46−48] The statistical methods were combined with direct SEM-EDS analysis in this paper. Manganese, Co, Ni, Cu, Zn, As, Mo, Cd, Cs, Tl, and Pb are positively correlated to the ash yield, total sulfur, and Fe_2O_3 (Figure 9), while they were negatively correlated to the total C and N content of the studied samples. Since they are either siderophile or chalcophile, it can be inferred that they were inorganically associated; therefore, pyrite is likely their main host. In contrast, Be, Sc, Cr, Ga, Ba, Ta, Bi, Th, U, and REEs are positively correlated to the ash yield; furthermore, most of them are significantly positively related to the lithophile elements SiO_2, Al_2O_3, MgO, K_2O, Na_2O, and TiO_2, suggesting that they mainly occurred in aluminosilicate minerals. However, Li, Sr, and Y show weakly negative correlations to both ash yield and total sulfur content.

5.1. Mode of Occurrence of Li. Lithium displays weak or no correlation with most other indices (including other elements, moisture, ash yield, and volatile, Figure 9). The correlation coefficients of Li-Al_2O_3, Li-Be, Li-Bi, and Li-Th are more than 0.5, while those of Li-S, Li-Fe_2O_3, Li-Co, Li-Ni, Li-Mo, and Li-Tl are less than −0.4 (Figure 9). Lithium, Al, Be, and Th are lithophiles, while Co, Ni, and Tl are siderophile or chalcophile elements. The correlation analysis of Li indicates it mainly occurred in the clay minerals, corresponding to the former studies[49] and the high percentage of clay minerals in C6 coal. Among the clay minerals in C6 coal, chlorite (chamosite) is an alternative host of Li in the formula of $(Mg,Fe^{2+},Fe^{3+},Mn,Ni,Na,Li,Al)_6[(Si,Al)_4O_{10}](OH)_8$,[49] which has been reported in Guanbanwusu coals as well.[50] Kaolinite is also a probable host of Li, which was been discovered in both Jincheng coals and Zhina coals.[14,23] I/S was the dominant clay mineral in the roof and floor samples (Table 4), which was also reported to have a relatively high Li concentration.[29] There is no doubt that I/S is one of the hosts of Li; however, it cannot be the major host of Li in the C6 coal samples because the coal samples have a much lower I/S content but a higher Li concentration than that of the roof and floor samples. Comparatively, kaolinite, rather than chlorite, is likely the dominant host of Li in C6 coal. The concentrations of Li are much higher in the samples with high kaolinite contents. Moreover, Li is significantly positively correlated with kaolinite while negatively correlated with chlorite and I/S (Figure 10b). Therefore, kaolinite is the major Li-bearing mineral in C6 coal.

Lithium is a critical metal in China, United States, the EU, and many other countries. Many attempts have been made to recover Li from coal ash.[4,19−22] Though there is a relatively high Li concentration in Chinese coals, it is still much lower than the Chinese industrial indicator for recovery of associated Li_2O (0.2%).[51] Only coals from a few coalfields, such as Jungar and Pingshuo coals, have reached the industrial indicator. Li_2O in the C6 coal ash ranges from 0.01 to 0.15%, which is lower than the industrial indicator. To reduce the costs of mining, the recovery cutoffs of Li in coals were proposed to be 100 and 120 μg/g.[4,52] Based on this threshold, Li in C6 coals (averaging 124 μg/g) is a potential extraction target.

5.2. Mode of Occurrence of Sr. Strontium occurs in minerals in the form of Sr^{2+}, so it is often hosted in carbonate, phosphate, sulfate, and silicate minerals.[49] Samples WJB-05 and WJB-06 are significantly rich in Sr. The concentrations of Sr were positively correlated to only CaO in C6 coals (Figure 9). In addition, samples WJB-05 and WJB-06 significantly influenced the correlations between Sr and CaO in C6 coal, indicating that Ca-bearing minerals were the main host of Sr in samples WJB-05 and WJB-06. Celestine was observed in sample WJB-05 in the SEM-EDS examination, and Ca and Ba were also detected in the sample (Figure 8e). Therefore, it can be reasonably inferred that celestine was one of the major Sr-bearing minerals in samples WJB-05 and WJB-06.

6. CONCLUSIONS

The Late Permian C6 coal in the Wenjiaba Mine is anthracite with a low ash yield, medium to high sulfur content, and low volatile yield. Mineralogical compositions are composed of clay minerals, pyrite, quartz, and calcite. Clay minerals, including kaolinite, chlorite, illite, and mixed-layer illite/smectite, are the major mineralogical components in C6 coal.

Contents of SiO_2, Al_2O_3, Fe_2O_3, MgO, TiO_2, K_2O, and CaO are lower than those in common Chinese coals, while Na_2O was higher. Lithium was significantly enriched in C6 coal, with an average of 124 μg/g, and it was dominantly hosted by kaolinite. Strontium was enriched in C6 coal as well, with an average of 663 μg/g, especially for samples WJB-05 and WJB-06, and dominantly occurred in the celestine.

AUTHOR INFORMATION

Corresponding Author

Fangpeng Du − *College of Geology and Environment, Xi'an University of Science and Technology, Xi'an 710054, China; Shaanxi Provincial Key Laboratory of Geological Support for Coal Green Exploitation, Xi'an 710054, China;* orcid.org/0000-0001-5741-9011; Email: dfp@xust.edu.cn

Authors

Shuzheng Ning − *China National Administration of Coal Geology, Beijing 100038, China*

Junwei Qiao − *College of Geology and Environment, Xi'an University of Science and Technology, Xi'an 710054, China; Shaanxi Provincial Key Laboratory of Geological Support for Coal Green Exploitation, Xi'an 710054, China;* orcid.org/0000-0002-7201-2663

Furong Tan − *China National Administration of Coal Geology, Beijing 100038, China; Shaanxi Institute of Geological Survey, Xi'an 710054, China*

Xiaochen Zhao − *College of Geology and Environment, Xi'an University of Science and Technology, Xi'an 710054, China; Shaanxi Provincial Key Laboratory of Geological Support for Coal Green Exploitation, Xi'an 710054, China*

Weiguo Zhang − *College of Geology and Environment, Xi'an University of Science and Technology, Xi'an 710054, China; Shaanxi Provincial Key Laboratory of Geological Support for Coal Green Exploitation, Xi'an 710054, China*

Congcong Li − *Aerophotogrammetry and Remote Sensing Bureau, China National Administration of Coal Geology, Xi'an 710199, China*

Zheng Luo − *Aerophotogrammetry and Remote Sensing Bureau, China National Administration of Coal Geology, Xi'an 710199, China*

Xiaoyuan He − *Aerophotogrammetry and Remote Sensing Bureau, China National Administration of Coal Geology, Xi'an 710199, China*

https://doi.org/10.1021/acsomega.0c05663
ACS Omega 2021, 6, 8816−8828

Complete contact information is available at:
https://pubs.acs.org/10.1021/acsomega.0c05663

Notes

The authors declare no competing financial interest.

■ ACKNOWLEDGMENTS

The authors thank the Geological survey Project of China Geological Survey (No. DD20160187), the National Natural Science Foundation of China (No. 41702144), and the Natural Science Basic Research Plan in Shaanxi Province of China (Nos. 2020JQ-743 and 2020JQ-746) for support.

■ REFERENCES

(1) Seredin, V. V.; Dai, S. Coal deposits as potential alternative sources for lanthanides and yttrium. *Int. J. Coal Geol.* **2012**, *94*, 67−93.
(2) Hower, J. C.; Eble, C. F.; Dai, S.; Belkin, H. E. Distribution of rare earth elements in eastern Kentucky coals: indicators of multiple modes of enrichment? *Int. J. Coal Geol.* **2016**, *160*−*161*, 73−81.
(3) Dai, S.; Finkleman, R. B. Coal as a promising source of critical elements: Progress and future prospects. *Int. J. Coal Geol.* **2018**, *186*, 155−164.
(4) Sun, Y.; Zhao, C.; Li, Y.; Wang, J. Minimum mining grade of the selected trace elements in Chinese coal. *Journal of China Coal Society* **2014**, *39*, 744−748.
(5) Bunt, J. R.; Waanders, F. B. Trace element behaviour in the Sasol−Lurgi MK IV FBDB gasifier. Part 1- the volatile elements: Hg, As, Se, Cd and Pb. *Fuel* **2008**, *87*, 2374−2387.
(6) Bunt, J. R.; Waanders, F. B. Trace element behaviour in the Sasol−Lurgi MK IV FBDB gasifier. Part 2 − the semi-volatile elements: Cu, Mo, Ni and Zn. *Fuel* **2009**, *88*, 961−969.
(7) Bunt, J. R.; Waanders, F. B. Trace element behaviour in the Sasol-Lurgi fixed-bed drybottom gasifier. Part 3 − the non-volatile elements: Ba, Co, Cr, Mn, and V. *Fuel* **2010**, *89*, 537−548.
(8) Bunt, J. R.; Waanders, F. B. Volatile trace element behaviour in the Sasol fixed-bed dry-bottom (FBDB) gasifier treating coals of different rank. *Fuel Process.Technol.* **2011**, *92*, 1646−1655.
(9) Wang, Y.; Tang, Y.; Guo, X.; Xie, Q.; Finkelman, R. B.; Li, P.; Chen, P. Fate of potentially hazardous trace elements during the entrained-flow coal gasification processes in China. *Sci. Total Environ.* **2019**, *668*, 854−866.
(10) Dai, S.; Li, T.; Seredin, V. V.; Ward, C. R.; Hower, J. C.; Zhou, Y.; Zhang, M.; Song, X.; Song, W.; Zhao, C. Origin of minerals and elements in the Late Permian coals, tonsteins, and host rocks of the Xinde Mine, Xuanwei, eastern Yunnan, China. *Int. J. Coal Geol.* **2014**, *121*, 53−78.
(11) Dai, S.; Seredin, V. V.; Ward, C. R.; Hower, J. C.; Xing, Y.; Zhang, W.; Song, W.; Wang, P. Enrichment of U−Se−Mo−Re−V in coals preserved within marine carbonate successions:geochemical and mineralogical data from the Late Permian Guiding Coalfield, Guizhou, China. *Miner. Deposita* **2015**, *50*, 159−186.
(12) Dai, S.; Xie, P.; Jia, S.; Ward, C. R.; Hower, J. C.; Yan, X.; French, D. Enrichment of U-Re-V-Cr-Se and rare earth elements in the Late Permian coals of the Moxinpo Coalfield, Chongqing, China: Genetic implications from geochemical and mineralogical data. *Ore Geol. Rev.* **2017**, *80*, 1−17.
(13) Tian, L.; Dai, S.; Wang, J.; Huang, Y.; Ho, S. C.; Zhou, Y.; Lucas, D.; Koshland, C. P. Nanoquartz in Late Permian C1 coal and the high incidence of female lung cancer in the Pearl River Origin area: a retrospective cohort study. *BMC Public Health* **2008**, *8*, No. 398.
(14) Li, B.; Zhuang, X.; Li, J.; Querol, X.; Font, O.; Moreno, N. Enrichment and distribution of elements in the Late Permian coals from the Zhina Coalfield, Guizhou Province, Southwest China. *Int. J. Coal Geol.* **2017**, *171*, 111−129.
(15) Wang, D.; Liu, L.; Liu, X.; Zhao, Z.; He, H. Main types and research trends of energy metallic resources in China *J. Guilin Univ. Technol.* 2016, 361 21 28. (In Chinese with English abstract).
(16) Miatto, A.; Reck, B. K.; West, J.; Graedel, T. E. The rise and fall of American lithium. *Resour., Conserv. Recycl.* **2020**, *162*, No. 105034.
(17) Ketris, M. P.; Yudovich, Y. E. Estimations of Clarkes for carbonaceous biolithes: world average for trace element contents in black shales and coals. *Int. J. Coal Geol.* **2009**, *78*, 135−148.
(18) Dai, S.; Ren, D.; Chou, C. L.; Frinkelman, R. B.; Seredin, V. V.; Zhou, Y. Geochemistry of trace elements in Chinese coals: A review of abundances, genetic types, impacts on human health, and industrial utilization. *Int. J. Coal Geol.* **2012**, *94*, 3−21.
(19) Dai, S.; Li, D.; Chou, C. L.; Zhao, L.; Zhang, Y.; Ren, D.; Ma, Y.; Sun, Y. Mineralogy and geochemistry of boehmite-rich coals: new insights from the Haerwusu Surface Mine, Jungar Coalfifield, Inner Mongolia, China. *Int. J. Coal Geol.* **2008**, *74*, 185−202.
(20) Sun, Y.; Zhao, C.; Li, Y.; Wang, J.; Liu, S. Li distribution and mode of occurrences in Libearing coal seam # 6 from the Guanbanwusu mine, Inner Mongolia, northern China. *Energy Explor. Exploit.* **2012**, *30*, 109−130.
(21) Ning, S.; Deng, X.; Li, C.; Qin, G.; Zhang, J.; Zhu, S.; Qiao, J.; Chen, L.; Zhang, W. Research status and prospect of metal element mineral resource in China *J. China Coal Soc.* 2017, *429* 2214 2225. (In Chinese with English abstract).
(22) Zou, J.; Han, F.; Tian, H. M.; Li, T.; Li, Y. Mineralogical and Geochemical composition of the Lopingian coals in the Zhongliangshan Coalfield, Southwestern China. *Minerals* **2018**, *8*, No. 104.
(23) Zhao, L.; Dai, S.; Nechaev, V. P.; Nechaeva, E. V.; Graham, I. T. Enrichment origin of critical elements (Li and rare earth elements) and a Mo-U-Se-Re assemblage in Pennsylvanian anthracite from the Jincheng Coalfield, southeastern Qinshui Basin, northern China. *Ore Geol. Rev.* **2019**, *115*, No. 103184.
(24) Dai, S.; Zhang, W.; Ward, C. R.; Seredin, V. V.; Hower, J. C.; Li, X.; Song, W.; Wang, X.; Kang, H.; Zheng, L.; Wang, P.; Zhou, D. Mineralogical and geochemical anomalies of late Permian coals from the Fusui Coalfield, Guangxi Province, southern China: Influences of terrigenous materials and hydrothermal fluids. *Int. J. Coal Geol.* **2013**, *105*, 60−84.
(25) Hower, J. C.; Campbell, J. L.; Teesdale, W. J.; Nejedly, Z.; Robertson, J. D. Scanning proton microprobe analysis of mercury and other trace elements in Fe-sulfides from a Kentucky coal. *Int. J. Coal Geol.* **2008**, *75*, 88−92.
(26) Karayigit, A. I.; Atalay, M.; Oskay, R. G.; Córdoba, P.; Querol, X.; Bulut, Y. Variations in elemental and mineralogical compositions of Late Oligocene, Early and Middle Miocene coal seams in the Kale-Tavas Molasse sub-basin, SW Turkey coal. *Int. J. Coal Geol.* **2020**, *218*, No. 103366.
(27) Seredin, V. V.; Dai, S.; Sun, Y.; Chekryzhov, I. Y. Coal deposits as promising sources of rare metals for alternative power and energy-effifficient technologies. *Appl. Geochem.* **2013**, *31*, 1−11.
(28) Finkelman, R. B. Modes of occurrence of hazardous elements in coal: level of confidence. *Fuel Process. Technol.* **1994**, *39*, 21−34.
(29) Frinkelman, R. B.; Palmer, C. A.; Wang, P. Quantification of the modes of occurrence of 42 elements in coal. *Int. J. Coal Geol.* **2018**, *185*, 138−160.
(30) Finkelman, R. B.; Dai, S.; French, D. The importance of minerals in coal as the hosts of chemical elements: A review. *Int. J. Coal Geol.* **2019**, *212*, No. 103215.
(31) Rudmin, M.; Ruban, A.; Savichev, O.; Mazurov, A.; Dauletova, A.; Savinova, O. Authigenic and Detrital Minerals in Peat Environment of Vasyugan Swamp, Western Siberia. *Minerals* **2018**, *8*, No. 500.
(32) Zhang, S.; Liu, C.; Hao, L.; Wang, J.; Bai, J.; Yang, M.; Liu, G.; Huang, H.; Guan, Y. Paleoenvironmental conditions, organic matter accumulation, and unconventional hydrocarbon potential for the Permian Lucaogou Formation organic-rich rocks in Santanghu Basin, NW China. *Int. J. Coal Geol.* **2018**, *185*, 44−60.
(33) Dai, S.; Zhang, W.; Seredin, V. V.; Ward, C. R.; Hower, J. C.; Song, W.; Wang, X.; Li, X.; Zhao, L.; Kang, H.; Zheng, C.; Wang, P.; Zhou, D. Factors controlling geochemical and mineralogical compositions of coals preserved within marine carbonate successions: A case study from the Heshan Coalfield, southern China. *Int. J. Coal Geol.* **2013**, *109*−*110*, 77−100.

(34) Karayiğit, A. I.; Littke, R.; Querol, X.; Jones, T.; Oskay, R. G.; Christanis, K. The Miocene of coal seams in the Soma Basin (W. Turkey): Insights from coal petrography and mineralogy and geochemistry. *Int. J. Coal Geol.* **2017**, *173*, 110−128.
(35) Karayiğit, A. I.; Bircan, C.; Oskay, R. G.; Türkmen, I.; Querol, X. The geology, mineralogy, petrography, and geochemistry of the Miocene Dursunbey coal within fluvio-lacustrine deposits, Balıkesir (Western Turkey). *Int. J. Coal Geol.* **2020**, *228*, No. 103548.
(36) Shi, R.; Shi, X.; Glasmacher, U. C.; Yang, X.; Stockli, D. F. The evolution of eastern Sichuan basin, Yangtze block since Cretaceous: Constraints from low temperature thermochronology. *J. Asian Earth Sci.* **2015**, *116*, 208−221.
(37) Xiao, L.; Xu, Y.; Mei, H.; Zheng, Y.; He, B.; Pirajno, F. Distinct mantle sources of low-Ti and high-Ti basalts from the western Emeishan large igneous province, SW China:implications for plume−lithosphere interaction. *Earth Planet. Sci. Lett.* **2004**, *228*, 525−546.
(38) Chen, R.; Yuan, K.; Zhang, Z.; Xu, Q.; et al. Sedimentary environment of organic-rich shale in the Upper Permian Longtan Formation in Qinglong area, western Guizhou, China. *China Geol.* **2019**, *1*, 108−109.
(39) Chinese standard GB/T 30732-2014, Proximate analysis of coal-Instrumental method, 2014. [in Chinese].
(40) Chinese standard GB/T 214-2007, Determination of total sulfur in coal, 2007. [in Chinese].
(41) Chinese petroleum industry standard SY/T 5163-2010, Analysis methods of clay minerals and ordinary non-clay minerals in sedimentary rocks by the X-ray diffraction, 2010. [in Chinese].
(42) Chinese standard GB/T 15224-2010, Classification for quality of coal, 2010. [in Chinese].
(43) Dai, S.; Seredin, V. V.; Ward, C. R.; Hower, J. C.; Xing, Y.; Zhang, W.; Song, W.; Wang, P. Enrichment of U-Se-Mo-Re-V in coals preserved within marine carbonate successions:geochemical and mineralogical data from the Late Permian Guiding Coalfield, Guizhou, China. *Miner. Deposita* **2015**, *50*, 159−186.
(44) Taylor, S. R.; McLennan, S. M. *The Continental Crust: Its Composition and Evolution*; Blackwell: Oxford, 1985; p 312.
(45) Dai, S.; Chou, C. L. Occurrence and origin of minerals in a chamosite-bearing coal of Late Permian age, Zhaotong, Yunnan, China. *Am. Mineral.* **2007**, *92*, 1253−1261.
(46) Dai, S.; Hower, J. C.; Finkelman, R. B.; Graham, I. T.; French, D.; Ward, C. R.; Eskenazy, D.; Wei, Q.; Zhao, L. Organic associations of non-mineral elements in coal: A review. *Int. J. Coal Geol.* **2020**, *218*, No. 103347.
(47) Eskanazy, G.; Finkelman, R. B.; Chattarjee, S. Some considerations concerning the use of correlation coefficients and cluster analysis in interpreting coal geochemistry data. *Int. J. Coal Geol.* **2010**, *83*, 491−493.
(48) Xu, N.; Finkelman, R. B.; Xu, C.; Dai, S. What do coal geochemistry statistics really mean? *Fuel* **2020**, *267*, No. 117048.
(49) Finkelman, R. B.; Dai, S.; French, D. The importance of minerals in coal as the hosts of chemical elements: A review. *Int. J. Coal Geol.* **2019**, *212*, No. 103215.
(50) Dai, S.; Jiang, Y.; Ward, C. R.; Gu, L.; Seredin, V. V.; Liu, H.; Zhou, D.; Wang, X.; Sun, Y.; Zou, J.; Ren, D. Mineralogical and geochemical compositions of the coal in the Guanbanwusu Mine, Inner Mongolia, China: Further evidence for the existence of an Al (Ga and REE) ore deposit in the Jungar Coalfield. *Int. J. Coal Geol. 98*, 10 40. DOI: 10.1016/j.coal.2012.03.003.
(51) DZ/T 0203-2002. *Geology and Ore Deposit Standard Specifications for Rare Metal Mineral Exploration of the People's Republic of China*; Geological Publishing: Beijing, p 40 (in Chinese).
(52) Yudovich, YaE.; Ketris, M. P. *Valuable Trace Elements in Coal*; RAS: Ekaterinburg, 2006.

https://doi.org/10.1021/acsomega.0c05663
ACS Omega 2021, 6, 8816−8828